Comparison of the Interactions of XeF_2 and F_2 with Si(100)(2 × 1)†

J. R. Holt, R. C. Hefty, M. R. Tate, and S. T. Ceyer*

Department of Chemistry, Massachusetts Institute of Technology, Cambridge, Massachusetts 02139

Received: April 9, 2002; In Final Form: June 10, 2002

The interaction of low-energy XeF_2 with Si(100)(2 × 1) has been studied and compared to that of F_2. Helium atom diffraction, beam-surface scattering, and thermal desorption measurements are the major techniques used in this study. It is found that XeF_2 dissociatively chemisorbs with high probability solely on the Si dangling bonds up to a coverage of about one monolayer (ML). Molecular fluorine has previously been observed to react similarly, saturating the dangling bonds at 1 ML coverage. The thermal desorption kinetics and products from the fluorinated layer produced by XeF_2 exposure are identical to those produced by F_2 exposure. The interactions of XeF_2 and F_2 are also strikingly similar with respect to the long-range order of the fluorinated Si up to about 1 ML coverage. The order is monitored by He diffraction. In both systems, the diffracted He beams exhibit a sharp decrease in intensity because of the disorder produced by the fluorination of random surface-unit cells as the coverage increases from 0 to about 0.3 ML. The intensity then increases until the fluorine overlayer has fully recovered its (2 × 1) periodicity at about 1 ML. This recovery corresponds to the decoration of each Si dangling bond with a fluorine atom. A critical observation of this study is that despite the large exothermicity of the dissociative chemisorption of XeF_2 or F_2 the order of the surface is not destroyed in either system. After saturation of the dangling bonds, F_2 ceases to react with the surface whereas XeF_2 continues to deposit fluorine by reacting with the Si−Si σ dimer bonds and the Si−Si lattice bonds. The order is destroyed as a result of the continued fluorine deposition, and ultimately, etching occurs by the formation of volatile SiF_4.

I. Introduction

The integration of conventional electronics with 3D mechanical components within a Si microchip is known as microelectromechanical systems technology or MEMS. The fabrication of these 3D mechanical structures involves many steps that may include X-ray lithography, chemical vapor deposition, and anisotropic chemical etching, but it also requires an isotropic etching step. One isotropic etchant currently in use is XeF_2.[1−5] Xenon difluoride is a gas-phase, plasmaless etchant that reacts rapidly and isotropically with Si at room temperature, neither leaving an adsorbed byproduct on nor radiatively damaging the Si. Its etching rates are as high as 40 μ/min. Among other advantages offered by XeF_2 is compatibility with complementary metal oxide semiconductor technology processing.[6]

Of interest in the present work is the high reactivity of XeF_2 with Si as compared to the reactivity of F_2. Given the chemical similarities of XeF_2 and F_2, it is curious that the reaction rate of XeF_2 with Si to form volatile etch products such as SiF_4 is 10^3-10^4 times higher than that of F_2.[7−11] In short, XeF_2 etches Si whereas F_2 does not. Since the discovery that XeF_2 spontaneously etches Si under ambient conditions,[7] many investigators have sought to understand why XeF_2 is so reactive with Si.[12−20] The vast majority of these investigations have been carried out with sufficient XeF_2 exposure to produce high fluorine coverages that yield the volatile etch product. In contrast, this investigation compares the interactions of XeF_2 and F_2 as the fluorine coverage builds from zero. It aims to delineate the fluorine coverage at which the interactions of XeF_2 and F_2 diverge. This goal is now possible because of recent extensive and quantitative studies of the mechanism and dynamics of the dissociative chemisorption of F_2 on Si(100)(2 × 1).[21−24] The results of these studies provide a means of calibrating the fluorine coverage. The calibration in turn enables the absolute probability of the dissociative chemisorption of XeF_2 and the coverage at which etching begins to be determined.

This investigation also aims to test the notion that the release of the exothermicity to Si upon XeF_2 dissociative chemisorption disorders the surface periodicity by introducing defects. Disorder is said to be responsible for the onset and subsequent high rates of XeF_2 etching.[25−28] This notion is curious because our previous work has shown that F_2 incident at low translational energies (<3.8 kcal/mol) on Si(100) reacts only with the Si dangling bonds. No disorder of the surface is evident, even though the dissociative chemisorption of F_2 on Si can be exothermic by as much as 251 kcal/mol.[21,22] Indeed, the absence of disorder upon the interaction of F_2 with Si and the absence of F_2 etching are consistent with the notion that disorder is a prerequisite for etching. However, consider the relative exothermicities of the interactions of F_2 and XeF_2 with Si. Although the dissociative chemisorption of XeF_2 is at least 28 kcal/mol *less* exothermic than the dissociative chemisorption of F_2, XeF_2 spontaneously etches Si whereas F_2 does not. It would be of interest to probe whether the dissociative chemisorption of XeF_2 induces disorder, in contrast to the behavior of the more exothermic interaction of F_2 on Si. The primary roadblock to an assessment of the structure of a fluorine overlayer is that the readily available technique, electron diffraction, is not suitable. The large electron-stimulated desorption cross section of fluorine leads to destruction of the overlayer before the structure can be determined. In this study, He atom diffraction is employed to monitor the structure of the fluorine overlayer as a function of exposure to

† Part of the special issue "John C. Tully Festschrift".

* Corresponding author. E-mail: stceyer@mit.edu.

10.1021/jp020936p CCC: $22.00 © 2002 American Chemical Society
Published on Web 07/10/2002

XeF_2 and F_2, thereby testing the notion that disorder resulting from defects is necessary for the onset of etching.

II. Experimental Section

The apparatus has been described in detail elsewhere.[29] Briefly, the apparatus consists of two differentially pumped molecular beam sources coupled to an ultrahigh vacuum chamber (base pressure of 5×10^{-11} Torr) housing the Si crystal, a cylindrical mirror energy analyzer for Auger spectroscopy, an ion-sputtering gun, a residual gas mass analyzer, and a triply differentially pumped, line-of-sight, rotatable quadrupole mass spectrometer. The spectrometer is equipped with a pseudorandom chopper, allowing for time-of-flight measurements.

A. Molecular Beams. The primary beam is a semieffusive expansion of neat XeF_2 (99% pure by F ion titration, Lancaster Synthesis) or F_2 (97% pure, Air Products, without HF trap). To avoid decomposition of the XeF_2 upon exposure to atmospheric gases, the XeF_2 is stored under nitrogen and transferred to a stainless steel vessel in a pressurized nitrogen glovebox. The stainless steel vessel is isolated and then attached to the gas-handling manifold leading to the beam source without exposing the XeF_2 to the atmosphere. Prior to each day's experiments, the XeF_2 beam is allowed to flow for 15 min. The manifold is then evacuated, and the process is repeated. This procedure serves to degas the XeF_2 sample and to passivate the walls of the stainless steel gas-handling manifold.[30] To achieve a constant stagnation pressure, the temperature of the stainless steel vessel containing the XeF_2 solid is held constant at 30(±1) °C by submerging it in a water bath. The remainder of the gas-handling manifold including the nozzle is also warmed to eliminate "cold spots" that would condense the XeF_2 vapor and cause the stagnation pressure to fluctuate. Consequently, the stagnation pressure is constant at 6.40 ± 0.04 Torr as measured by a Baratron capacitance manometer. The neat F_2 is taken directly from the gas cylinder and regulated at a stagnation pressure of 6.4 Torr to match the XeF_2 stagnation pressure. The beams used in most of the experiments presented here are expanded from a $4.7(\pm 0.8) \times 10^{-9}$ m^2 orifice of a Ni nozzle and are subsequently passed through a single differential pumping region, with collimating slits located at the entrance and exit of the differential stage. The average translational energies of the XeF_2 and F_2 beams formed in this fashion are 1.95 ± 0.07 and 1.63 ± 0.05 kcal/mol, respectively, as measured by cross-correlation time-of-flight spectroscopy. The corresponding full energy widths at half-maximum are 2.30 and 1.99 kcal/mol, respectively. Beams of XeF_2 and F_2 with average translational energies of 1.29 and 1.32 kcal/mol were also used in some experiments. The results are independent of these small changes in incident energy.

Determination of the absolute beam flux is detailed elsewhere.[22] Briefly, a beam of Ar at a stagnation pressure of 6.40 ± 0.04 Torr is directed into the chamber containing the crystal. The pressure rise in the chamber, P, is measured with a nude Bayard−Alpert ionization gauge and calibrated to the absolute pressure by accounting for the ionization efficiency, C, of Ar. The absolute flux of Ar impinging on an area, A, of the crystal is given by $I^{Ar} = PCS/kTA$, where S is the pumping speed of Ar and T is the temperature of the chamber. The flux of a beam of pure F_2 or XeF_2 at a stagnation pressure of 6.40 ± 0.04 Torr is given by $I = I^{Ar}v/v^{Ar}$, where v and v^{Ar} are the experimentally determined average speeds of F_2 or XeF_2 and Ar, respectively. Because there are two F atoms per molecule in both F_2 and XeF_2, the incident flux in terms of F atoms is I [F atoms/m^2 s] $= 2I^{Ar}v/v^{Ar}$. This procedure yields values of 0.097(±0.005) and 0.16(±0.01) ML F atom/s for the flux of the incident XeF_2 and F_2 beams, respectively, where 1 ML is the surface density of Si atoms on a Si(100) surface, 6.78×10^{14} atoms/cm^2.

The secondary source is aimed at the crystal so that its beam is at a 20° angle from the primary beam. The secondary beam is a supersonic expansion of 300 Torr of a mixture of 75% He (99.9999%, Spectra Gases)/25% Ar (99.9995%, Spectra Gases) through a 0.002-in. diameter orifice held at 320 ± 20 K. This expansion results in nearly monoenergetic He atoms with an average translational energy of 21.4 meV (fwhm = 13.3 meV) and a 0.93-Å de Broglie wavelength. This beam is used for He diffraction measurements.

B. Si(100) Crystal. The lightly p-doped Si(100) crystal is mounted between two Ta clamps that are attached to the manipulator. The Ta clamps are flush with the crystal face, thereby eliminating the possibility of spurious shadowing effects of the crystal surface by the beams incident at glancing angles. The crystal can be cooled to 125 K and heated resistively to ~1100 K, as measured via a W-5%Re/W-26%Re thermocouple clamped to the back of the crystal. The temperature is held constant at 250 K during XeF_2 or F_2 exposure. The temperature is stabilized using a proportional integral differential (PID) feedback loop to control the resistive-heating power supply. Similar results to those shown below are obtained after XeF_2 or F_2 exposure of Si(100) at 150 and 300 K.

The Si crystal is cut along the (100) plane and cleaned by a wet-etching procedure[31] prior to installation into the vacuum chamber. The crystal is mounted such that the scattering plane, defined by the beams, crystal normal, and detector, is along the (10) direction of the crystal surface. Helium diffraction confirms the (2 × 1) periodicity of the reconstructed Si(100) surface. The crystal is cleaned by sputtering with 1.5-keV Ar^+ followed by a 30-min. anneal at 1100 K. This process is repeated until carbon and oxygen contamination are below the 1% sensitivity limit of Auger electron spectroscopy. No metal contamination, such as W, Ta, Cu, or Ni, is observed. Between experiments, a brief anneal at 1100 K is used to clean the surface and restore the (2 × 1) surface periodicity. A heating rate of 2 K/s and a cooling rate of 0.7 K/s is used for all anneals. The crystal is replaced when an etch spot becomes visible, typically after several months of experiments. No difference in the reactivity or the diffraction spectra of the Si(100) crystal is observed over the lifetime of the crystal.

C. Detection Scheme. Thermal desorption and scattering measurements employ a triply differentially pumped, rotatable quadrupole mass spectrometer with electron bombardment ionization as the detector. The detector rotates in the plane of the beams around their point of intersection at the crystal surface. The angular range of the detector is 35° to 180.5° with respect to the primary beam. Its angular resolution in the scattering plane is 3.52°. It has been shown that the use of a properly differentially pumped detector is critical, in particular for the detection of radical species such as SiF_2. Spurious features due to secondary interactions of the radical species with the chamber walls can obfuscate the signal of the radical species scattered directly from the surface.[22]

III. Results

A. Dissociative Chemisorption Probability of XeF_2 on Si(100) at 250 K. Recent studies of the interaction of F_2 with Si(100)(2 × 1) have shown that F_2 reacts via atom abstraction with the Si(100) surface dangling bonds. Once each dangling bond is bound to a F atom, the reaction ceases. The resulting

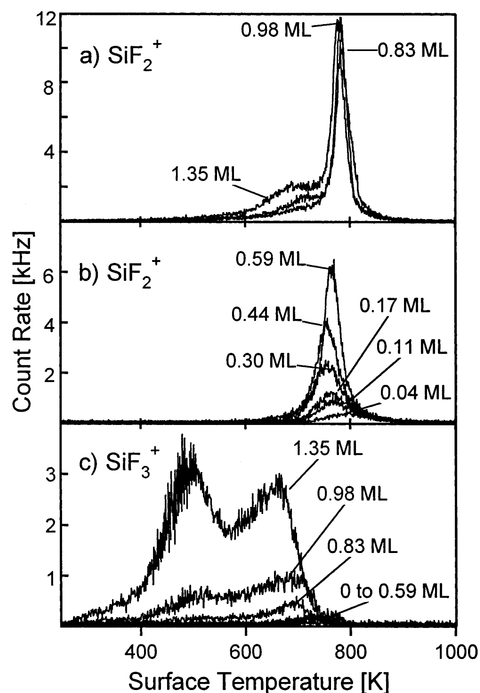

Figure 1. Thermal desorption spectra measured at $m/e = 66$ (a, b) and $m/e = 85$ (c) after XeF_2 exposure at $T_s = 250$ K to yield the fluorine coverages in ML F atoms that are shown for each trace. Temperature ramp rate is 5 K/s.

saturation coverage is about 1 ML (0.94 ± 0.11).[22] The partial pressures of products desorbing from this layer that are monitored in a thermal desorption experiment and that are integrated over temperature are a measure of 1 ML of adsorbed fluorine. This value is used in the present study to calibrate the fluorine coverage resulting from a known exposure of Si(100) to XeF_2. Knowledge of this fluorine coverage coupled with knowledge of the absolute flux of the incident XeF_2 beam enables the dissociative chemisorption probability of XeF_2 to be determined as a function of coverage, as follows.

The crystal is held at 250 K during exposure to a beam of F_2 or XeF_2. The beam is incident 20° to the normal of the crystal surface. The crystal is subsequently rotated so that its normal is aligned with the axis of the differentially pumped mass spectrometer. The crystal temperature is then increased at a rate of 5 K/s, and the masses at $m/e = 66$ (SiF_2^+) and $m/e = 85$ (SiF_3^+) are monitored. The SiF_2^+ and SiF_3^+ signals originate from the ionization or dissociative ionization of the SiF_2 and SiF_4 parent molecules, respectively, in agreement with previous results.[32] Figure 1 shows typical thermal desorption spectra measured after exposure to XeF_2, resulting in a variety of fluorine coverages measured in monolayers, where 1 ML is equivalent to one F atom per Si surface atom. The fluorine coverage determination is described below. The major product, SiF_2, is observed as a single feature around 800 K. The SiF_2 desorption rate exhibits second-order kinetics as the coverage increases to 0.30 ML. Above 0.30-ML F atom coverage, the SiF_2 desorption rate is zeroth order. Desorption of the minor product SiF_4 is observed as two broad features around 500 and 700 K in Figure 1c. These desorption products and kinetics are essentially identical to those that have been previously reported for the interaction of F_2 with Si(100).[24] The thermal desorption traces for the F_2 system are not shown here. However, unlike the behavior observed in the F_2 system, desorption of SiF_2 and SiF_4 are observed for coverages greater than 1 ML, as shown in Figures 1a and c, because, as explained below, the dissociative

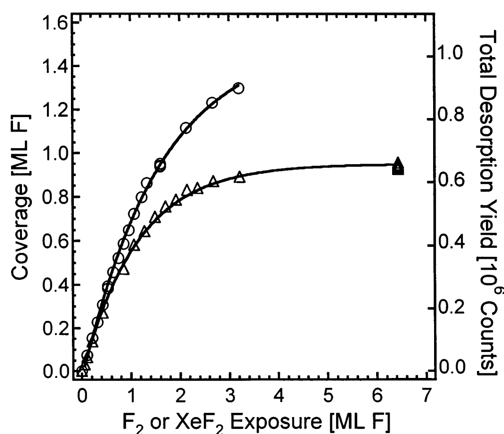

Figure 2. Total thermal desorption yield (right axis) and fluorine coverage in ML F atoms (left axis) as a function of exposure to F_2 (△) and XeF_2 (○) in ML F atoms. See text for explanation of axes. Solid lines are exponential fits to the data.

chemisorption probability of XeF_2 does not approach zero as the coverage increases to 1 ML.

The total thermal desorption yield at a given exposure or coverage is the sum of the SiF_2 and SiF_4 signals in Figure 1 integrated over temperature.[24] Briefly, the integrated yields of each product are scaled for the relative detection sensitivities of SiF_2 and SiF_4, the factor of 2 more fluorine atoms that SiF_4 has relative to SiF_2, the different velocity and angular distributions of the desorbing SiF_2 and SiF_4 species, and their relative ionization cross sections and quadrupole transmissions. The SiF_4 thermal desorption yield as a result of exposure to XeF_2 is small, never exceeding 9% of the SiF_2 yield.

The total thermal desorption yield, in arbitrary units, is plotted on the right-hand abscissa in Figure 2 as a function of exposure to XeF_2 and F_2. Both yields increase steadily as the exposure increases from 0 to 1 ML of F atoms, but beyond this exposure, the yield resulting from exposure to F_2 becomes constant whereas the yield resulting from exposure to XeF_2 continues to increase. Because the fluorine saturation coverage as a result of exposure to F_2 is known to be 0.94 ± 0.11 ML,[22] the abscissa on the left-hand side has been calibrated such that the average of the total yields of the nine highest F_2 exposures (6.5-ML F atom exposure) is 0.94 ± 0.11 ML. With this calibration, it is clear that the fluorine coverage resulting from exposure to XeF_2 increases beyond the approximately 1 ML saturation coverage achieved by exposure to F_2. This observation implies that the dissociative chemisorption probability of XeF_2 on Si(100) covered by 1 ML of fluorine is not equal to zero.

There is a second important difference between the interaction of XeF_2 and F_2 with Si(100) at 250 K. For sufficiently long exposures to XeF_2, the fluorine that adsorbs does not have an infinitely long residence time at 250 K. Instead, the fluorine desorbs as the volatile etch product, SiF_4. This desorption is seen in Figure 3a, which is a plot of the signal at $m/e = 85$ (SiF_3^+), corresponding to SiF_4, as a function of exposure to XeF_2. The XeF_2 beam is incident 20° from the normal whereas the mass spectrometer detector is positioned 15° from the normal. The ordinate in Figure 3a is converted from exposure to coverage by means of a calibration similar to that shown in Figure 2. The resulting plot of the etch product as a function of fluorine coverage is shown in Figure 3b. For coverages lower than 0.7 ML, negligible etch product is formed, whereas between 0.8 and 1.0 ML, the amount of desorbing SiF_4 grows rapidly. Beyond 1.0 ML, the observed etch product remains essentially constant. Observation of this etch product is in striking contrast

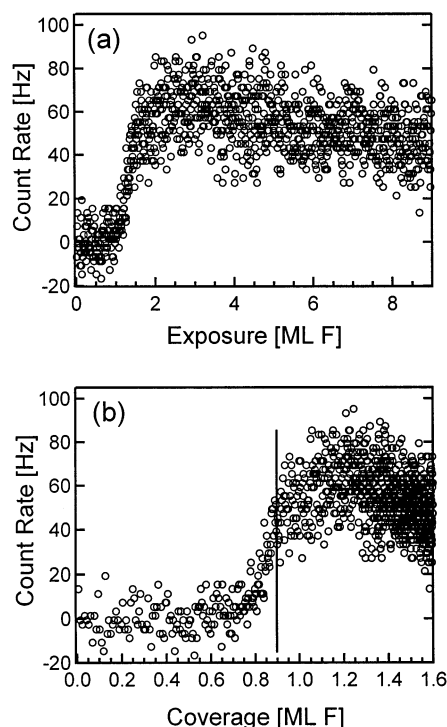

Figure 3. SiF_3^+ (m/e = 85) signal (average of data from five experiments) as a function of (a) exposure and (b) coverage during exposure to XeF_2. The XeF_2 beam is incident at $\theta_i = 20°$, and the detector is at $\theta_d = 15°$ with respect to the normal. The line marks the onset of etching.

to the interaction of F_2 with Si(100), a system in which no etching is observed when F_2 is incident on Si(100) at 250 K.[22]

The dissociative chemisorption probability of XeF_2 and F_2 as a function of fluorine coverage is calculated from the derivatives of the plots in Figure 2. An exponential function given by

$$\text{coverage [ML]} = 0.950 - 0.970e^{-0.885\epsilon} \qquad \text{for } F_2 \quad (1)$$

$$\text{coverage [ML]} = 2.26 - 2.28e^{-0.362\epsilon} \qquad \text{for } XeF_2 \quad (2)$$

is fit to the measurements of coverage as a function of XeF_2 or F_2 exposure in ML F atoms, ϵ, in Figure 2. The derivative of these functions with respect to exposure yields the dissociative chemisorption probability as a function of exposure or coverage. The dissociative chemisorption probability as a function of coverage is plotted in Figure 4. Dissociative chemisorption probabilities for XeF_2 are calculated only for coverages below about 0.8 ML because probabilities determined by this thermal desorption method are valid only when the residence time of the adsorbate is effectively infinite. As discussed above with reference to Figure 3, during exposure to XeF_2, the fluorine begins to desorb as SiF_4 as the fluorine coverage builds to 0.8 ML. More precisely, the probability plotted in Figure 4 represents the sum $0.5P_1 + P_2$, where P_1 is the probability for single-atom abstraction and P_2 is the probability for two-atom adsorption. Single-atom abstraction refers to the abstraction of a single F atom from an incoming F_2 or XeF_2 molecule by a Si dangling bond, yielding the complementary fragments F or XeF, respectively, scattered into the gas phase. Two-atom adsorption refers to the abstraction of one F atom from the incident F_2 or XeF_2 followed by the adsorption of the complementary F atom in the case of F_2 or the abstraction of the second F atom from the complementary XeF fragment in the case of XeF_2. A more

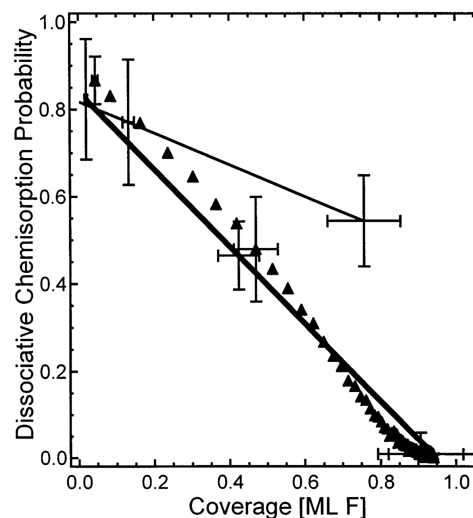

Figure 4. Dissociative chemisorption probability ($0.5P_1 + P_2$) calculated from the derivative of the exponential fits in Figure 2. The thick and thin lines show the derivative of the exponential fits with respect to F_2 and XeF_2 exposure, respectively, plotted vs coverage. The solid triangles show $0.5P_1 + P_2$ adapted from ref 22. Note that above ~0.8 ML XeF_2 exposure produces the SiF_4 etch product, so the probability cannot be determined by this method. Error bars are 95% confidence limits and are the propagated errors resulting from the uncertainties of the fit in Figure 2 of the beam flux and of the saturation coverage given in ref 22.

detailed explanation of the definition of the dissociative chemisorption probability is given in the discussion of eq IV.11 in ref 22. The definition of the dissociative chemisorption probability is not of consequence in the present work. It is only of consequence when comparing its value to literature values of this quantity.[33,34]

Our previous determination of the quantity $0.5P_1 + P_2$ by a scattering method[22] for the interaction of F_2 with Si(100) has been included for comparison in Figure 4. There is good agreement between the F_2 dissociative chemisorption probability that is measured as described here and the measurements made by a scattering method. The F_2 dissociative chemisorption probability decreases rapidly with increasing coverage, approaching zero at 0.94 ± 0.11 ML, the saturation coverage. In contrast, the XeF_2 probability is weakly dependent on coverage, decreasing to only about 0.6 at 0.8 ML coverage, the coverage at which etching begins to occur.

B. Surface Structure Determination by He Atom Diffraction. Previous reports have detailed the He atom diffraction technique with regard to the reconstructed Si(100) surface[35] and, specifically, its application to the fluorinated surface.[24] Si(100) reconstructs by forming rows of surface Si dimers, resulting in one partially filled molecular orbital or dangling bond projecting into the vacuum for each surface Si atom. The distance between equivalent Si atoms in adjacent dimers in the same row is the same as the lattice spacing, whereas the distance between equivalent Si atoms in dimers from adjacent rows is twice the lattice spacing, resulting in a (2 × 1) surface unit cell that is observable by He diffraction.

The characteristic He diffraction spectrum arising from this reconstructed surface is shown in Figure 5a as a function of angle from the surface normal. All He diffraction spectra are measured from a surface at 250 K with the He beam incident 40° from the surface normal. The scattered He signal is presented in Figure 5a with no background subtraction. The resulting spectrum consists of specular, half-order, and first-order diffraction features, as indicated in Figure 5a. The broad

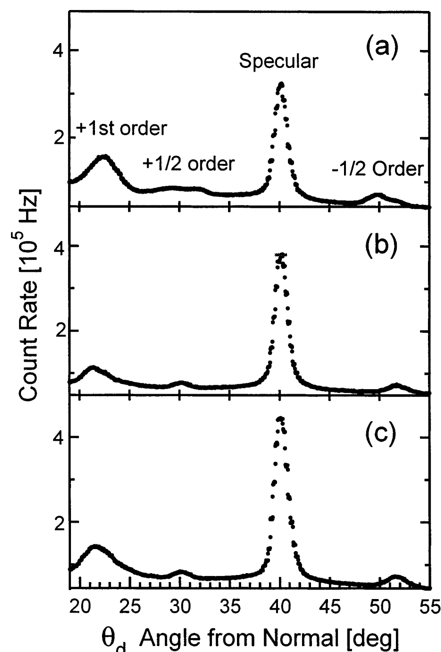

Figure 5. Helium signal scattered from Si(100) at 250 K and at $\theta_i = 40°$ as a function of the detector angle θ_d: (a) clean surface; (b) 0.9 ML coverage resulting from F_2 exposure; and (c) 0.9 ML coverage resulting from XeF_2 exposure. Each point represents a measurement made with a dwell time of 2 s and at angular intervals of 0.25°. Error bars on the He atom count rate are smaller than the width of each point.

width of the diffraction features is a consequence of the large acceptance angle of the detector, which was chosen to optimize the intensity of the reactively scattered signal rather than the angular resolution of the elastically scattered signal. The widths of these features can be reproduced well in a simulation that convolutes the finite size of the incident beam and the detector chamber entrance slits with the distribution of velocities of the incident beam.[36] The intensity of the specular feature is quite sensitive to disorder produced by any kind of defect and is used in this study as a measure of the overall surface order. The half-order diffraction feature arises from the periodic doubling of the lattice spacing in the direction perpendicular to the dimer rows. It is therefore a signature for the presence of Si dimers and is used in this study as an indicator of the cleavage of Si−Si σ dimer bonds upon the adsorption of fluorine. The first-order feature arises from diffraction parallel to the dimer rows.

The Si dangling bonds, which are effectively radical sites and hence very reactive species, are the logical sites for F atom reaction. It has been reported that F_2 reacts solely at the dangling bonds on the Si(100) surface and that no Si−Si lattice bonds or σ dimer bonds are broken.[24] Shown in Figure 5b is a He diffraction spectrum of the Si surface after sufficient exposure to F_2 to saturate the dangling bonds. Although the intensities of the features are changed upon fluorination from that of a clean surface, the (2 × 1) periodicity persists. The reaction produces a fully fluorinated and well-ordered Si(100)(2 × 1) surface where no Si−Si bonds have been broken, the Si dimers remain intact, and each surface Si atom is decorated with a single fluorine atom. F_2 does not etch the Si surface.[22]

A He diffraction spectrum measured after exposure of Si(100) to 1.5-ML F atom of XeF_2, which yields a coverage of 0.9 ML, is shown in Figure 5c. The diffraction spectrum measured after this exposure to XeF_2 is nearly identical to the spectrum measured after F_2 exposure in Figure 5b! The dimer rows are intact, as indicated by the persistence of the (2 × 1) periodicity, and at 0.9 ML coverage, almost every surface Si atom is decorated with a single fluorine atom. Despite its superior etching ability and large reaction exothermicity, XeF_2 has not induced any significant disorder of the surface, even though XeF_2 has reacted sufficiently to cover the surface with 0.9-ML F atoms.

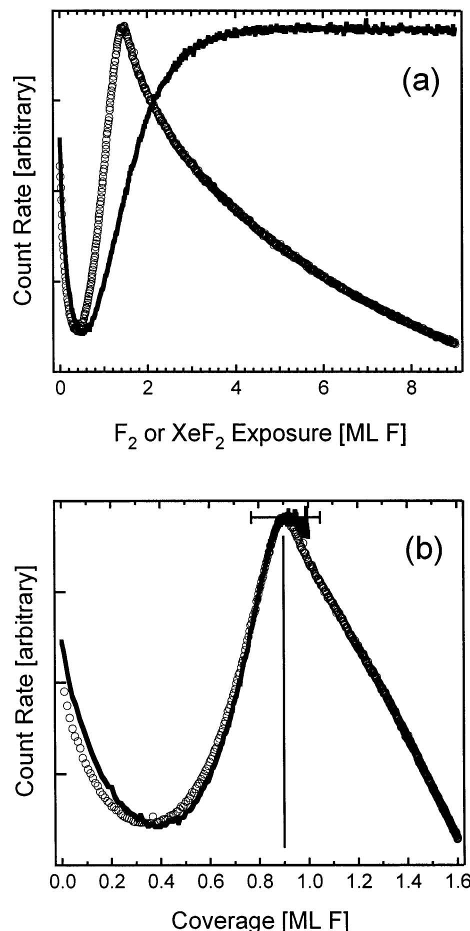

Figure 6. Intensity of the specular He diffraction feature as a function of (a) exposure and (b) coverage during exposure to F_2 (●) and XeF_2 (○). The He beam is incident at $\theta_i = 40°$, and the F_2 or XeF_2 beam is incident at $\theta_i = 20°$. The detector is positioned at $\theta_d = 40°$. Signals have been normalized at the maximum intensity of each trace. Error bars on the He atom count rate are smaller than the width of each point. The line marks the coverage at which the scattered He signal is a maximum.

Whereas this experiment provides a snapshot of the fluorine overlayer at a single coverage, it is informative to probe the surface periodicity as the fluorine overlayer evolves. To do so, the intensities of the He diffraction features are monitored as a function of F_2 or XeF_2 exposure. The He probe beam is incident at 40° with respect to the surface normal, while the F_2 or XeF_2 reactant beam is simultaneously incident at 20° with respect to the normal. The differentially pumped mass spectrometer is positioned 40° from the normal angle in the forward scattering direction. The intensity of the specular feature is then monitored by the mass spectrometer as a function of exposure. Figure 6a shows the evolution of the specular feature with respect to exposure of Si(100) to both F_2 and XeF_2. The maximum intensities of both traces have been normalized. Figure 6b shows the same evolution of the intensity of the specular feature plotted with respect to coverage. The coverage at a given exposure is calculated from expressions such as those given in eqs 1 and 2. The intensity of the specular feature decays rapidly during the initial exposure of the surface to both F_2 and XeF_2. This initial loss of intensity can be understood in terms

of fluorination of the surface at random sites. The presence of a F atom bonded to a dangling bond changes the interaction potential of the He atom with that surface unit cell, thereby making it different from the surrounding unit cells that do not yet include a F atom. The surface order is disrupted, thus resulting in a loss of coherency of the diffracted He beam.[24,37] The specular intensity reaches a minimum at about 0.35 ML and then begins to recover. This recovery signals the transition to a new order as the periodicity of the fluorinated surface unit cells begins to predominate over that of the unfluorinated unit cells. Eventually, the original (2 × 1) periodicity is recovered, indicating that most of the dangling bonds are fluorinated and that most unit cells are fluorinated identically to their neighbors. The intensity of the specular feature fully recovers at 0.9 ± 0.1 ML coverage, corresponding to F_2 and XeF_2 exposures of 3−5 and 1.3-ML F atoms, respectively. The uncertainty in the coverage arises from the propagated uncertainty in the fit of the thermal desorption signal and the uncertainty of the previously reported determination of the saturation coverage.[22]

The recovery of the specular feature at a coverage that is slightly below 1 ML, where the surface is more fully ordered, can be understood in terms of the limited transfer width of the apparatus. As discussed elsewhere in detail,[24] the transfer width of the apparatus is estimated to be 35 Å, which means that ordered regions of the surface greater than 35 Å in length will not contribute to the intensity of the diffracted beams.[38] That is, once the ordered regions of the surface have surpassed this size, the intensity of the diffracted beam will remain constant as the coverage increases. However, for microscopic 2D ordering below the transfer width of the apparatus, the He diffracted intensities are extremely sensitive to surface disorder. As apparent in Figure 6b, the He diffraction technique is sensitive to the surface disorder produced by a change in coverage of as little as 0.01 ML.

Figure 6 shows that in the submonolayer coverage regime, there is a striking similarity between F_2 and XeF_2. In fact, up to 0.9 ML coverage, it would be extremely difficult to distinguish between the two reactants solely on the basis of the evolution of the surface order. However, beyond 0.9 ML, the reactivities differ greatly. The intensity of the specular feature remains essentially constant upon further exposure to F_2 because the F_2 dissociative chemisorption probability becomes effectively zero, as shown in Figure 4. In contrast, the intensity of the specular feature decreases rapidly upon further exposure to XeF_2, indicating that the periodicity is rapidly destroyed.

The half-order and first-order diffraction features were also monitored as a function of coverage during exposure to XeF_2. The half-order feature is of interest because it arises from the periodicity of the dimer rows and hence is visible only when the dimer bonds are intact. It is used in this study as an indicator of the cleavage of Si−Si σ dimer bonds upon the adsorption of fluorine. The He probe beam is incident at 40° with respect to the surface normal, while the F_2 or XeF_2 reactant beam is simultaneously incident at 20° with respect to the normal. The intensities of the first- and half-order features are monitored by the differentially pumped mass spectrometer positioned 21.5° and 51.25°, respectively, from the normal in the forward scattering direction. The evolution of these features, whose intensities are normalized, as a function of coverage resulting from XeF_2 exposure is shown in Figure 7. Both features show the characteristic initial decrease caused by random fluorination, recovery at 0.9 ML, and subsequent decay. The decay of both features beyond 0.9 ML is evidence for the destruction of the (2 × 1) periodicity and hence the cleavage of the Si−Si σ dimer

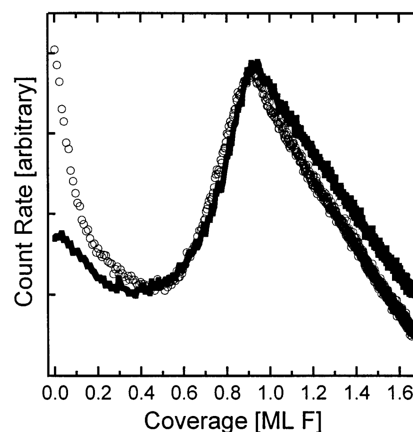

Figure 7. Intensity of the +1 order (●) and −1/2 order (○) He diffraction features as a function of coverage during exposure to XeF_2. The He beam is incident at $\theta_i = 40°$, the F_2 or XeF_2 beam is incident at $\theta_i = 20°$, and the detector is positioned at $\theta_d = 21.5°$ (+1 order) or 51.25° (−1/2 order). Signals have been normalized at the maximum intensity of each trace. Error bars on the He atom count rate are smaller than the width of each point.

and Si−Si lattice bonds because of continued reaction with XeF_2. Indeed, the dissociative chemisorption probability of XeF_2 remains high at 0.9 ML, as shown in Figure 4. In addition, the onset of desorption of the etch product, SiF_4, is observed at this coverage, as shown in Figure 3. Clearly, in contrast to the interaction of F_2 with 1 ML of F adsorbed on Si(100), XeF_2 reacts at this coverage, depositing additional fluorine while cleaving Si−Si bonds. The additional fluorine and the desorption of the etch product lead to disordering of the surface, as evident from He atom diffraction.

IV. Discussion

This study has shown that dissociative chemisorption of XeF_2 proceeds in a manner identical to that of F_2 as the coverage increases from 0 to about 1 ML on Si(100)(2 × 1). Figure 6b shows that the intensity of the specular He diffraction feature as a function of fluorine coverage produced by the dissociative chemisorption of XeF_2 is indistinguishable in this coverage regime from that produced by the dissociative chemisorption of F_2. Both XeF_2 and F_2 dissociatively chemisorb initially by reacting solely with dangling bonds at random sites, leading to a loss of coherence of the zeroth-order diffraction beam. As the coverage increases and more unit cells are fluorinated, the coherence of the specular beam recovers, and its intensity is maximized at about 0.9 ML for both XeF_2 and F_2. Diffraction spectra measured from a fluorinated surface at 0.9 ML coverage over a wide angular range are shown in Figures 5b and c for the F_2 and XeF_2 systems, respectively. The spectra reveal that the fluorinated surface is well-ordered with a (2 × 1) periodicity. The dimer rows remain intact, with each surface Si atom decorated with a fluorine atom. The only difference between XeF_2 and F_2 in this coverage regime is that the chemisorption probability of XeF_2 decreases slowly as the coverage approaches 1 ML whereas that of F_2 decreases rapidly and is effectively zero at 1 ML, as shown in Figure 4. The relative constancy of a chemisorption probability with coverage is usually interpreted in terms of a long lifetime of an extrinsic precursor, which is a species physisorbed on top of filled sites.[39] An extrinsic precursor diffuses on top of the filled sites until it encounters an empty site, such as a dangling bond, and reacts or desorbs without dissociating. In short, the extrinsic precursor makes it more likely that a XeF_2 molecule will encounter an unoccupied

dangling bond and hence increases the dissociation probability.[11] The substantially greater polarizability of XeF_2 compared to that of F_2 suggests that a XeF_2 extrinsic precursor would have a longer lifetime than that of F_2. A second explanation for the relative constancy of the dissociative chemisorption probability is the longer collision time of XeF_2 compared to that of F_2. Because it is 4 times more massive than F_2, XeF_2 spends twice as long as F_2 in the near-surface region where it may encounter an unoccupied dangling bond. It is not clear from the present study if either effect or both effects are operative.

Once the dangling bonds are saturated at about 1 ML coverage, the interactions of XeF_2 and F_2 differ dramatically. Whereas the reaction of F_2 with Si(100) essentially ceases, XeF_2 continues to chemisorb dissociatively, as indicated by the increase in fluorine coverage beyond 1 ML in Figure 2. Chemisorption of fluorine beyond 1 ML requires cleavage of the Si−Si σ dimer bonds, the Si−Si lattice bonds, or both. The simultaneous decay of both the first- and half-order diffraction features provides evidence that the cleavage of both types of Si−Si bonds is occurring. The concomitant cleavage of Si−Si bonds and formation of Si−F bonds leads to disorder of the surface periodicity, as indicated by the decay of the specular, first-, and second-order diffraction features as the coverage increases beyond 1 ML. The increased fluorine coverage results in the formation of more highly fluorinated species such as SiF_2 and SiF_3. These species have been identified in XPS measurements of Si(100) at approximately 1.5 ML coverage.[40−42] They eventually form the SiF_4 that desorbs. In short, XeF_2 etches the Si surface, but F_2 does not.

Clearly, the dangling-bond sites on the Si(100) surface are by far the dominant sites for the dissociative chemisorption of XeF_2, just as they are for F_2.[27,43,44] Previous work has demonstrated that the mechanism for dissociative chemisorption of F_2 is atom abstraction. The cross section for F atom abstraction from F_2 by the dangling bonds is measured to be large compared to the cross sectional area of a surface site.[23] The large cross sections suggest the presence of an attractive interaction potential that is consistent with the notion of molecular steering.[45,46] Recent work has also provided direct evidence for atom abstraction in the XeF_2/Si(100) system.[47] Upon saturation of the dangling bonds, the only sites available for reaction are ones that involve cleavage of Si−Si bonds. An F_2 molecule incident at thermal energies does not react with these sites. In fact, it has been shown that a barrier to that reaction of 3.8 kcal/mol exists.[24] This barrier can be surmounted by translational activation of F_2. In contrast, it is apparent that no such barrier exists in the case of XeF_2. The XeF_2 molecule that is incident at thermal energies reacts readily with these sites.

An important point demonstrated by this study is that the exothermicity released to the surface upon dissociative chemisorption of XeF_2 or F_2 below about 1 ML coverage does not destroy the surface order, in contrast to the conclusions given in previous work.[25−28] It is also clear that the presence of disorder is not a precondition for etching to begin. Clearly, XeF_2 begins to react with the Si−Si bonds in the presence of an ordered overlayer of fluorine. It is the reaction of XeF_2 with these Si−Si bonds that leads to the disorder of the surface periodicity rather than the disorder induced by the exothermicity release that leads to the reaction of XeF_2 with the Si−Si bonds.

We have shown that the reaction of low-energy XeF_2 with the Si(100)(2 × 1) reconstructed surface occurs solely at the Si dangling bonds up to a fluorine coverage of 0.9 ML. No Si−Si bonds are broken, and the ordered (2 × 1) reconstruction is preserved. The presence of the half-order feature at 0.9 ML coverage provides evidence that even the Si−Si σ dimer bonds are undisturbed, preserving the original dimer rows. Up until 0.9 ML, the reaction of XeF_2 with Si is remarkably similar to the reaction of F_2, especially considering the fact that their steady-state etch rates differ by 4 orders of magnitude. However, after saturation of the dangling bonds, F_2 ceases to react with the surface, but XeF_2 continues to deposit fluorine on the surface by reacting with the Si−Si bonds. The surface order is destroyed as a result of the continued fluorine deposition, and ultimately, etching occurs by the formation of volatile SiF_4.

Acknowledgment. This work is supported by NSF CHE-0091810. We thank D. L. Lahr for critically reading the manuscript.

References and Notes

(1) Ressejac, I. C.; Landsberger, L. M.; Currie, J. F. *J. Vac. Sci. Technol., A* **2000**, *18,* 746.

(2) Tea, N. H.; Milanović, V.; Zincke, C. A.; Suehle, J. S.; Gaitan, M.; Zaghloul, M. E.; Geist, J. *J. Microelectromech. Syst.* **1997**, *6*, 363.

(3) Chang, F. I.; Yeh, R.; Lin, G.; Chu, P. B.; Hoffman, E.; Kruglick, E. J. J.; Pister, K. S. J.; Hecht, M. H. *Proc. SPIE 1995 Symp. Microelectronic Struct. Microelectromech. Devices* **1995**, *2641*, 117.

(4) Chu, P. B.; Chen, J. T.; Yeh, R.; Lin, G.; Huang, J. C. P.; Warneke, B. A.; Pister, K. S. J. *Transducers 97, Proc. Int. Conf. Solid-State Sens. Actuators* **1997**, *97*, 665.

(5) Toda, R.; Minami, K.; Esashi, M. *Transducers 97, Proc. Int. Conf. Solid-State Sens. Actuators* **1997**, *97,* 671. *Sens. Actuators, A* **1998**, *66*, 268.

(6) Kovacs, G. T. A.; Maluf, N. I.; Petersen, K. E. *Proc. IEEE* **1998**, *86,* 1536.

(7) Winters, H. F.; Coburn, J. W. *Appl. Phys. Lett.* **1979**, *34*, 70.

(8) Mucha, J. A.; Donnelly, V. M.; Flamm, D. L.; Webb, L. M. *J. Phys. Chem.* **1981**, *85*, 3529.

(9) Flamm, D. L.; Donnelly, V. M.; Mucha, J. A. *J. Appl. Phys.* **1981**, *52*, 3633.

(10) Vasile, M. J. *J. Appl. Phys.* **1983**, *54*, 6697.

(11) Ibbotson, D. E.; Flamm, D. L.; Mucha, J. A.; Donnelly, V. M. *Appl. Phys. Lett.* **1984**, *44,* 1129.

(12) Winters, H. F.; Coburn, J. W. *Surf. Sci. Rep.* **1992**, *14*, 165.

(13) Tu, Y. Y.; Chuang, T. J.; Winters, H. F. *Phys. Rev. B* **1981**, *23*, 823.

(14) Haring, R. A.; Haring, A.; Saris, F. W.; de Vries, A. E. *Appl. Phys. Lett.* **1982**, *41*, 174.

(15) Vugts, M. J. M.; Hermans, L. J. F.; Beijerinck, H. C. W. *J. Vac. Sci. Technol., A* **1996**, *14*, 2138. Vugts, M. J. M.; Hermans, L. J. F.; Beijerinck, H. C. W. *J. Vac. Sci. Technol., A* **1996**, *14*, 2820.

(16) Chuang, T. J. *J. Chem. Phys.* **1981**, *74*, 1461.

(17) Houle, F. A. *J. Chem. Phys.* **1983**, *79*, 4237. Houle, F. A. *J. Chem. Phys.* **1984**, *80*, 4851.

(18) Houle, F. A. *Appl. Phys. Lett.* **1987**, *50*, 1838. Houle, F. A. *Phys. Rev. Lett.* **1988**, *61*, 1871. Houle, F. A. *Phys. Rev. B* **1989**, *39*, 10120.

(19) Li, B.; Streller, U.; Krause, H. P.; Twesten, I.; Schwentner, N. *J. Appl. Phys.* **1995**, *77*, 350.

(20) Aliev, V. S.; Kruchinin, V. N. *Surf. Sci.* **1999**, *442*, 206.

(21) Li, Y. L.; Pullman, D. P.; Yang, J. J.; Tsekouras, A. A.; Gosalvez, D. B.; Laughlin, K. B.; Zhang, Z.; Schulberg, M. T.; Gladstone, D. J.; Ceyer, S. T. *Phys. Rev. Lett.* **1995**, *74*, 2603. Ceyer, S. T. *Proc. R. A. Welch Found. Conf. Chem. Res. XXXVIII: Chemical Dynamics of Transient Species*; Welch Foundation: Houston, TX, 1994; pp 156−172. Pullman D. P.; Ceyer, S. T. *Abstr. Pap. Am. Chem. Soc.* **1994**, *207*, 168.

(22) Tate, M. R.; Gosalvez-Blanco, D.; Pullman, D. P.; Tsekouras, A. A.; Li, Y. L.; Yang, J. J.; Laughlin, K. B.; Eckman, S. C.; Bertino, M. F.; Ceyer, S. T. *J. Chem. Phys.* **1999**, *111*, 3679.

(23) Tate, M. R.; Pullman, D. P.; Gosalvez-Blanco, D.; Tsekouras, A. A.; Li, Y. L.; Ceyer, S. T. *J. Chem. Phys.* **2000**, *112*, 5190.

(24) Pullman, D. P.; Tsekouras, A. A.; Li, Y. L.; Yang, J. J.; Tate, M. R.; Gosalvez-Blanco, D.; Laughlin, K. B.; Schulberg, M. T.; Ceyer, S. T. *J. Phys. Chem. B* **2001**, *105*, 486.

(25) Lo, C. W.; Varekamp, P. R.; Shuh, D. K.; Durbin, T. D.; Chakarian, V.; Yarmoff, J. A. *Surf. Sci.* **1993**, *292*, 171.

(26) Simpson, W. C.; Yarmoff, J. A. *Surf. Sci.* **1996**, *359*, 135.

(27) Weakliem, P. C.; Carter, E. A. *J. Chem. Phys.* **1993**, *98*, 737.

(28) Carter, L. E.; Khodabandeh, S.; Weakliem, P. C.; Carter, E. A. *J. Chem. Phys.* **1994**, *100*, 2277.

(29) Ceyer, S. T.; Gladstone, D. J.; McGonigal, M.; Schulberg, M. T. In *Physical Methods of Chemistry*, 2nd ed.; Rossiter, B. W., Baetzold, R. C., Eds., Wiley & Sons: New York, 1993; Vol. IXA, p 383.

(30) Qiu, S. R.; Yarmoff, J. A. *Phys. Rev. B* **2001**, *63*, 115409.
(31) Ishizaka, A.; Shiraki, Y. *J. Electrochem. Soc.* **1986**, *133*, 666.
(32) Winters, H. F.; Houle, F. A. *J. Appl. Phys.* **1983**, *54*, 1218.
(33) Engstrom, J. R.; Nelson, M. M.; Engel, T. *Surf. Sci.* **1989**, *215*, 437.
(34) Behringer, E. R.; Flaum, H. C.; Sullivan, D. J.; Masson, D. P.; Lanzendorf, E. J.; Kummel, A. C. *J. Phys. Chem.* **1995**, *99*, 12863.
(35) Cardillo, M. J.; Becker, G. E. *Phys. Rev. B* **1980**, *21*, 1497.
(36) Yang, J. J. Ph.D. Thesis, Massachusetts Institute of Technology, Cambridge, MA, 1997.
(37) Poelsema, B.; Comsa, G. *Scattering of Thermal Energy Atoms from Disordered Surfaces*; Springer-Verlag: Berlin, 1989.
(38) Comsa, G. *Surf. Sci.* **1979**, *81*, 57.
(39) Kisliuk, P. *J. Phys. Chem. Solids* **1957**, *3*, 95.
(40) Chuang, T. J. *J. Appl. Phys.* **1980**, *51*, 2614.
(41) McFeely, F. R.; Morar, J. F.; Shinn, N. D.; Landgren, G.; Himpsel, F. J. *Phys. Rev. B* **1984**, *30*, 764.
(42) Shinn, N. D.; Morar, J. F.; McFeely, F. R. *J. Vac. Sci. Technol. A* **1984**, *2*, 1593.
(43) Stillinger, F. H.; Weber, T. A. *Phys. Rev. Lett.* **1989**, *62*, 2144. *J. Chem. Phys.* **1990**, *92*, 6239.
(44) Schoolcraft, T. A.; Garrison, B. J. *J. Vac. Sci. Technol., A* **1990**, *8*, 3496.
(45) Gostein, M.; Sitz, G. O. *J. Chem. Phys.* **1997**, *106*, 7378.
(46) Darling, G. R.; Kay, M.; Holloway, S. *Surf. Sci.* **1998**, *400*, 314.
(47) Ceyer, S. T. To be submitted for publication.